

Thermal Stability of Specialty Optical Fibers

Andrei A. Stolov, Debra A. Simoff, and Jie Li

Abstract—Application of silica optical fibers at elevated temperatures is limited by the thermal stability of their polymer coatings, as thermal degradation in most polymer materials occurs at much lower temperatures than silica, which can result in degradation in the fiber performance. In this paper, we attempt to clarify the concept of thermal stability of specialty polymer-coated silica optical fibers and demonstrate a quantitative measurement method using thermogravimetric analysis (TGA) in combination with methods for optical and strength measurement of optical fiber. Based on the results, long-term use temperatures for various specialty optical fibers are estimated.

Index Terms—Attenuation, coating, continuous use temperature, lifetime, optical fiber strength, optical fibers, polymer degradation, thermal stability, thermogravimetric analysis, upper use temperature.

I. INTRODUCTION

THE term “specialty optical fibers” is used to distinguish those fiber types that are designed or used outside the high-volume telecommunications realm. Specialty fibers may be exposed to harsh environments at high temperatures, such as for down-hole sensing in oil wells, high-power laser delivery, aerospace, and steam sterilization for medical use. When planning to use specialty optical fibers or cables at elevated temperatures, it is important to know how thermally stable they are. For silica glass optical fibers, the most vulnerable part is their polymer coatings. UV-curable dual acrylate coatings, used in most conventional optical fibers for long-distance communications, essentially enabled the practical use of silica glass optical fiber [1]–[3]. The soft primary (inner) coating prevents microbending, while the harder secondary (outer) coating provides abrasion resistance and mechanical robustness [4]. Advantages of such coatings include fast cure, avoidance of volatile solvents, ease of mechanical stripping with minimal residue, and low cost. A perceived shortcoming of such coatings in some specialty applications is their upper use temperature: conventional dual acrylate fibers are typically “rated” for 85 °C.

For higher-temperature applications, thermally cured coatings such as RTV silicones or polyimides are more commonly used. These polymer materials function well at temperatures up to 200 °C, and polyimides can be used even above 300 °C for short durations. Thermally cured coatings, although more

heat resistant, can be more difficult to strip for fiber termination. Also, their raw materials are more costly and their manufacturing processes are more complicated, involving solvent removal or control of limited pot life. They have slower cure rates, requiring lower fiber draw speeds, which increases cost.

Yet another class of specialty fiber coatings is UV cured fluoroacrylates. These are used primarily because of their low refractive index, where the coating also serves as an optical cladding. Fluoroacrylates tend to have heat resistance that is intermediate between that of conventional dual acrylates and polyimides.

As specialty optical fibers are being used in an increasingly wider variety of applications, clear definition of their thermal stability becomes necessary. It is not sufficient to merely describe “operation temperature” or “use temperature” without specifying the context of actual applications. In this paper, we analyze various aspects of thermal stability including thermal response of coatings and their impact on fiber properties and propose an approach for its quantitative evaluation that allows us to define the concept more completely. The approach is applied to specialty optical fibers with several classes of coatings.

II. THERMAL STABILITY

The term “thermal stability” may have a different meaning depending on the application of a particular polymer, coating or a product comprising those materials [5], [6]. For optical fibers used within telecommunications, fiber reliability testing is guided by industry standards such as ITU-T G.652, IEC60793-2, Telcordia GR-20-CORE and TIA/EIA-492. Dry heat aging may involve conditioning of fibers for 1 month at 85 °C [7]. However, a rating of 85 °C is not intended to convey suitability for continuous long-term use at 85 °C; rather, 85 °C is the short-term test temperature used to accelerate and simulate decades of exposure in outdoor terrestrial environments, such as Miami or Arizona, where the maximum operating temperature may be ~ 45 °C. For specialty fiber in higher-temperature applications, comprehensive industry standards have yet to be developed.

For an end user of a specialty optical fiber, it is necessary to know the highest temperature at which the fiber can function for a given duration of time, or equivalently, how the fiber’s performance changes as a function of temperature and time. There are three essential elements in defining thermal stability of a specialty optical fiber. They are: fiber performance, use temperature, and duration or lifetime. For all practical purposes, we may define the thermal stability of specialty optical fiber as the highest temperature at which the optical fiber retains its acceptable performance level for a specific duration, e.g., 20 years. The acceptance criteria for fiber performance must be defined based on the application of particular fibers. However, it is safe

Manuscript received January 15, 2008; revised April 04, 2008. Current version published December 19, 2008. **Disclaimer:** The predictions herein are based on the latest techniques of accelerated testing. Although as such, they may provide an indication of the useful service life of materials, they do not constitute or imply any warranty on behalf of OFS. No warranties other than OFS’ normal contractual warranties should be inferred.

The authors are with the Specialty Photonics Division, OFS, Avon, CT 06001 USA (e-mail: stolov@ofsoptics.com).

Digital Object Identifier 10.1109/JLT.2008.925698

to say that, for most specialty optical fiber users, thermal stability of optical and mechanical performance (e.g., attenuation and strength) of the fibers are most relevant. Thus, it is important to realize that the thermal stability of a fiber is really the thermal stability of the most relevant properties of the fiber, although dictated primarily by the thermal resistance of its polymer coatings.

Once the acceptance criteria are known, there are two questions that the fiber user should ask: 1) How long can a particular fiber operate at a certain (known) temperature and 2) What is the highest temperature at which the fiber can be used during a certain (known) time?

A similar concept is used by Underwriters Laboratories to determine the Relative Temperature Index (RTI), the maximum service temperature for a material where specific properties are not unacceptably compromised [8]. More than one RTI may be appropriate for a material depending on the property requirements for a given application. Different RTI values may be determined based on, e.g., electrical insulating properties, mechanical impact, and/or tensile properties.

At elevated temperatures (> 85 °C), when a fiber is exposed to an oxygen-containing environment, the coating degrades mostly due to thermooxidation [9], [10]. The oxidation reaction destroys the crosslinked network of the coating, mainly via scission of bonds, followed by loss of volatile by-products. A direct method of studying the material degradation is thermogravimetric analysis (TGA). In this method, the coating weight is determined as a function of time and temperature. Weight loss measurements can be performed at various temperatures and/or heating rates and in different environments (e.g., nitrogen, air, or oxygen), and only small samples (a few milligrams) are required. As will be described below, the TGA data obtained in a certain time-temperature range can be extrapolated to a broader range of times and temperatures. With the fiber performance tested separately under similar acceleration conditions, we can readily establish a link between it and the TGA data. Once the relationship is established, TGA provides a quantitative method of evaluating the thermal stability of optical fibers.

Thus, the analysis of thermal stability includes the following steps. 1) Defining the performance acceptance criteria. 2) Conducting accelerated aging tests of the fiber at elevated temperature(s) up to its failure. 3) Performing TGA analysis of the coating in an appropriate temperature range. 4) Correlating the fiber failure with coating weight loss. 5) Estimating the appropriate time-temperature range for the fiber application based on extrapolations of the TGA data.

III. TGA APPROACH

There are two main TGA approaches to lifetime determination: isothermal and dynamic. In the isothermal method, the sample is rapidly heated to a preset temperature and then is maintained at this temperature [11]–[13]. From the obtained TGA curve, the time of say 5% weight loss can be determined. Repeating the test at various temperatures, an extrapolation to other time frames (e.g., 20 years) can be made. In theory, the isothermal approach should be the most accurate one. However,

it has two significant shortcomings: long observation time and inevitable weight loss before reaching the observation temperature [12], [14], [15]. That is why the alternative (dynamic) approach is typically utilized.

In dynamic TGA, the sample is heated at a constant rate while its mass is being measured [16]–[22]. The decomposition kinetics parameters are then calculated within a framework of a certain model. All such models are based on the following general equation:

$$\frac{d\alpha}{dt} = k \cdot f(\alpha) = A \exp\left(-\frac{E^*}{RT}\right) f(\alpha) \quad (1)$$

where T is temperature, t is time, α is conversion or fractional weight loss (i.e., 0 in the beginning and 1 when all of the decomposed material is gone), k is the rate constant, A and E^* are the Arrhenius frequency factor and the activation energy, respectively, R is the gas constant and $f(\alpha)$ is a kinetic model function. Since $f(\alpha)$ is usually unknown, various mathematical functions are considered based on nucleation, geometrical, diffusion mechanism or reaction order concepts [23]–[27].

Using different approximations, the activation energy, and sometimes A and $f(\alpha)$, can be determined from the TGA data obtained at a single or multiple heating rates. The most widely used approaches were developed by Horowitz and Metzger [28], Coats and Redfern [29], Broido [30], Ozawa [31], Flynn and Wall [32], Kissinger [33] and Friedman [34]. Often, conflicting results are obtained using different approaches [24], [35]–[39]. The main reason for the discrepancy between the methods is that all of the models assume a single mechanism responsible for the thermal decomposition in the temperature range under study (i.e., only one set of A , E^* and $f(\alpha)$ in (1)). Generally speaking, this should not be true for optical fiber coatings, since their formulations involve different chemical ingredients. In particular, the single mechanism assumption cannot be completely valid for dual-coating systems.

As an alternative to the existing methods, we propose a more straightforward approach for evaluating the coating lifetime. As was indicated above, the fiber acceptance criteria must be defined. We make an assumption that the failure of fiber performance corresponds to a certain weight loss, $F\%$. As examples, we consider below the $F\%$ magnitudes of 5, 10, 25, or 50% coating weight loss. Mild weight loss generally corresponds to evaporation of volatile components, such as additives, non-reacted monomers or adsorbed moisture. Greater weight loss tends to indicate breakdown of the material. While we will discuss weight change here in terms of weight loss, weight can also increase somewhat upon heating (i.e., samples heated in air or oxygen can react with the oxygen in ways that increase their weight). Both oxygen uptake (weight gain) and weight loss can occur at the same time. Weight loss tends to be more evident at high temperatures, where evaporation rate is greater than the rate of oxygen incorporation.

Next, for assessing the lifetime, we determine the temperatures at two weight losses $X\%$ and $Y\%$ that are near $F\%$ (see Fig. 1). It is preferred that both $X\%$ and $Y\%$ belong to the range $[0 - F\%]$, so that the weight loss kinetics within the interval $X\% - Y\%$ represent some average over the range $[0 - F\%]$.

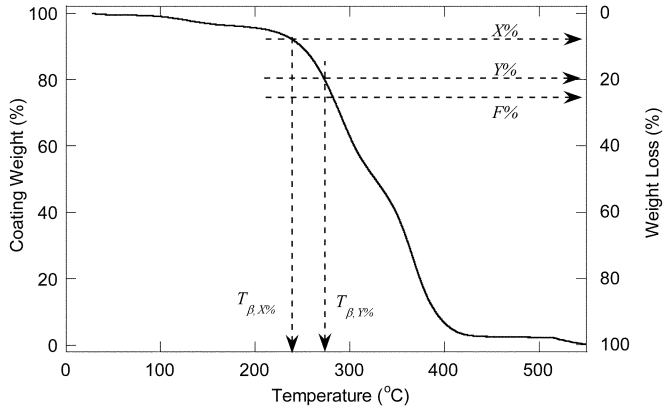


Fig. 1. Dynamic TGA thermogram obtained for Coating A in nitrogen at a heating rate of 0.5 °C/min. The dashed lines and notations explain the approach of assessing the material lifetime.

For instance, when $F = 25\%$, good magnitudes for $X\%$ and $Y\%$ would be 10 and 20%, respectively.

For a certain heating rate β , one can determine the temperatures at the weight losses of $X\%$ and $Y\%$. We denote these temperatures as $T_{\beta, X\%}$ and $T_{\beta, Y\%}$ (Fig. 1). Note that it is inconvenient to take $X\%$ equal or too close to zero, since at that condition the sample weight changes slowly, so that $T_{\beta, X\%}$ would be determined with a large uncertainty.

Going from $X\%$ to $Y\%$, the sample loses $(Y\% - X\%)$ of its weight during the time τ_{XY}

$$\tau_{XY} \approx \frac{dt}{dT} (T_{\beta, Y\%} - T_{\beta, X\%}) = \frac{(T_{\beta, Y\%} - T_{\beta, X\%})}{\beta}. \quad (2)$$

This weight loss time corresponds to some average temperature over the range $T_{\beta, X\%}$ to $T_{\beta, Y\%}$

$$T_{av} = \frac{(T_{\beta, Y\%} + T_{\beta, X\%})}{2}. \quad (3)$$

Thus, the time for the weight loss of $F\%$ at a given constant rate of loss at the average temperature can be calculated using a simple proportion

$$\tau_F \approx \tau_{XY} \cdot \frac{F}{(Y - X)}. \quad (4)$$

We assume Arrhenius behavior of τ_F

$$\ln \tau_F = \ln \tau_{F0} + \frac{E^*}{RT_{av}} \quad (5)$$

where $\ln \tau_{F0}$ is a pre-exponential. We next obtain the E^* and τ_{F0} values by plotting $\ln \tau_F$ versus $1/T_{av}$. Then, this plot can be extrapolated to other time-temperature conditions.

The advantage of the proposed approach is that it enables lifetime prediction in the most direct way, without relying on any decomposition model. It determines the effective pre-exponential and the activation energy that correspond to some averaged magnitudes for all decomposition reactions that occur in the considered weight loss region. In an ideal case, when thermal decomposition is governed by a single chemical reaction, our approach should provide data consistent with the isothermal and

various dynamic ones [11], [28]–[34] (that is, if the dynamic approaches use the correct model function).

Another advantage of our approach is that it enables one to verify the prediction quality by applying equations of regression analysis [40]. In addition to the linear correlation coefficient, the extrapolation error can be calculated. We plot the data in the Arrhenius coordinates, i.e.,

$$\zeta = a\xi + b \quad (6)$$

where $\zeta = \ln \tau_F$, $\xi = 1/T$, $a = E^*/R$ and $b = \ln \tau_{F0}$. At a certain value of ξ , the value of ζ is determined with a measure of uncertainty called the “confidence interval.” We calculate 95% confidence intervals using the following equation:

$$\zeta = a\xi + b \pm S \cdot t_{95\%, n-2} \left\{ \frac{1}{n} + \frac{(\xi - \xi_{mean})^2}{\sum_i (\xi_i - \xi_{mean})^2} \right\}^{1/2} \quad (7)$$

where S is a square root of the mean square about the regression (i.e., standard deviation of the experimental points with respect to the fit), n is the number of experimental points, $t_{95\%, n-2}$ is the Student coefficient, ξ_i is an i th measured value of ξ ($i = 1 \dots n$) and ξ_{mean} is the mean of the experimental magnitudes ξ .

When the experimental points fall well on a straight line, this leads to a relatively small extrapolation error. In contrast, when the experimental points do not fall well on a straight line (for instance if the Arrhenius plot systematically curves, indicating that the effective activation energy depends on the heating rate), this leads to an increase of the confidence interval for the extrapolated magnitude of $\ln \tau_F$.

IV. EXPERIMENTAL

A. Samples

Three fibers were drawn, having the following structure:

Fiber A has a 50 μm graded-index core and 125 μm diameter silica cladding. It has a dual acrylate coating (Coating A) with primary and secondary coating diameters of 190 and 245 μm , respectively. The numerical aperture for the fiber is 0.2.

Fiber B has a 200 μm pure silica core and 225 μm fluoroacrylate polymer cladding with a numerical aperture of 0.37. The polymer cladding on this fiber also plays a role of the coating (Coating B).

Fiber C is a single mode fiber with 125 μm cladding and 155 μm polyimide coating (Coating C). The numerical aperture of the fiber is 0.11.

B. TGA Testing

All thermogravimetric measurements were performed using a TA Instruments TGA 2950 thermogravimetric analyzer over a temperature range from ambient to 800 °C. The samples were small (< 1 cm) pieces of fiber placed in a platinum pan. Typical sample weight was in the region 10–40 mg. The sample chamber was purged using nitrogen, oxygen or air at a flow rate of 60 cm^3/min . The dynamic TGA experiments were performed at heating rates of 0.5, 1, 2, 5, 10, and 20 °C/min.

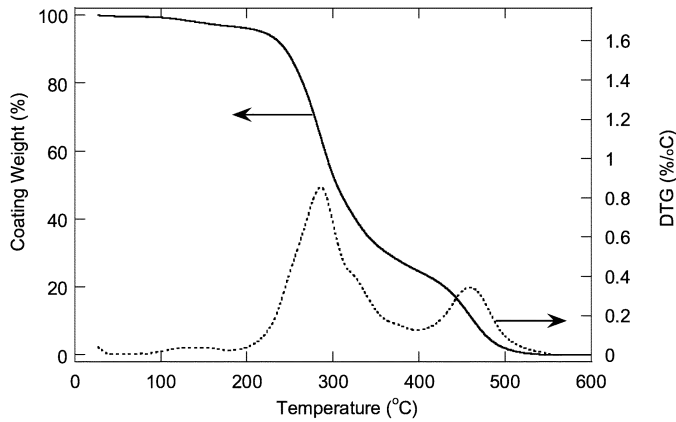


Fig. 2. Dynamic TGA curve (continuous line) and its temperature derivative (dashed line) obtained for Coating A in air at a heating rate of $1\text{ }^{\circ}\text{C}/\text{min}$.

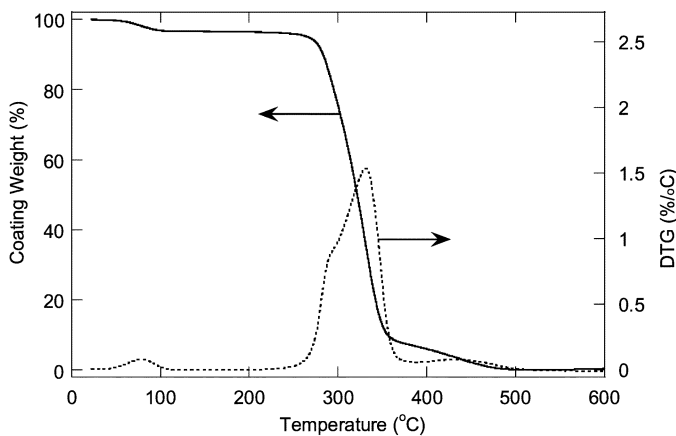


Fig. 3. Dynamic TGA curve (continuous line) and its temperature derivative (dashed line) obtained for Coating B in air at a heating rate of $1\text{ }^{\circ}\text{C}/\text{min}$.

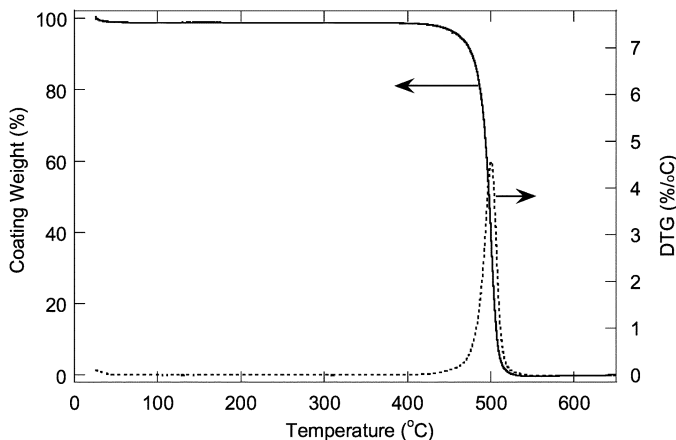


Fig. 4. Dynamic TGA curve (continuous line) and its temperature derivative (dashed line) obtained for Coating C in oxygen at a heating rate of $1\text{ }^{\circ}\text{C}/\text{min}$.

Since only the coating weight was of interest, we have subtracted the weight of the glass from the total weight measured by TGA. The weight fraction of the glass was determined from the residual weight of the samples at the highest experimental temperature ($800\text{ }^{\circ}\text{C}$). With the nitrogen purge, the coatings do not decompose completely even at $800\text{ }^{\circ}\text{C}$. To avoid this problem,

we switched the gas to oxygen at $650\text{ }^{\circ}\text{C}$ and then ramped to $800\text{ }^{\circ}\text{C}$ at $20\text{ }^{\circ}\text{C}/\text{min}$.

C. Fiber Aging

The thermal stability of Fiber A was also investigated using accelerated aging followed by measurements of coating diameter, fiber strength and optical attenuation. For the accelerated aging, the fiber was placed in an oven (Isotemp Temperature Programmable Oven, Model 818F, Fisher Scientific).

In preparation for strength and diameter tests, short ($< 20\text{ cm}$) straight lengths of fiber were hung vertically to minimize contact with each other and with other surfaces. The upper ends of the fibers were affixed to aluminum bars using Kapton polyimide tape. The oven was set at $300\text{ }^{\circ}\text{C}$, and the aging times were 5 and 30 min, and 24, 50, and 72 h. The oven temperature calibration was checked at both $250\text{ }^{\circ}\text{C}$ and $300\text{ }^{\circ}\text{C}$ and was found to agree within $\pm 3\text{ }^{\circ}\text{C}$ of the set point at most locations within the oven cavity.

D. Fiber Optical Tests

For the attenuation test, a loose fiber coil (1000 m long) was placed in a 10×14 aluminum tray and coated with talc before the aging. The specimen was placed inside an environmental chamber with the connectorized ends exiting through the chamber porthole and connected to a Rifocs optical transmittance system. The Rifocs system comprises 751R-850 LED light sources and a 676RE multichannel power meter. Optical transmittance at 850 nm was monitored throughout the test.

E. Fiber Coating Diameter Measurements

Coated fiber diameters were measured after aging using a TLaser 222 diameter gage. One $\sim 8\text{-cm}$ sample was examined from each aging condition. Each aged sample was measured three times, taking readings at its top, middle, and bottom (granted that the coating was still present). Fibers were centered in the detector crosshairs before readings to ensure measurement at the same reference point.

F. Fiber Strength Tests

The fiber strength was tested using a two-point bend technique with a Fiber Sigma 2 Point™ Bend Apparatus at a strain rate of $4\%/ \text{min}$ and ambient conditions. Details of the method can be found elsewhere [41], [42]. For the “as drawn” and aged fibers 10 specimens were tested per aging condition.

V. RESULTS AND DISCUSSION

A. Thermogravimetric Analysis

Typical dynamic TGA curves obtained for Coatings A, B, and C in air are given in Figs. 2–4. The dashed curves show the temperature derivatives (DTG). Each peak on the DTG curve corresponds to a certain weight loss mechanism. At relatively low temperatures ($< 200\text{ }^{\circ}\text{C}$), small broad peaks are observed for Coatings A and B. Those peaks are attributed to removal of uncrosslinked volatiles from the coating, rather than to network breakdown. Thermal decomposition predominates at higher temperatures.

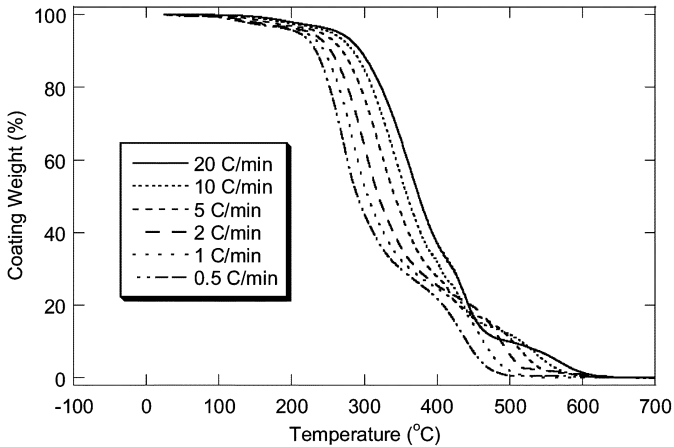


Fig. 5. Dynamic TGA curves obtained for Coating A in air at different heating rates.

Chemical reactions that occur during thermal decomposition are not necessarily known. Among studied coatings, Coating A represents the most complex case for TGA, since its DTG curve contains two strong peaks (at ~ 280 and ~ 470 °C), and the former peak also reveals two shoulders (at ~ 250 and 330 °C). It follows that the decomposition of Coating A includes at least four different steps. In contrast, the decomposition of Coating C exhibits a single narrow DTG peak, which should represent the easiest case for analysis.

Examples of the dynamic TGA curves obtained at different heating rates for Coating A are shown in Fig. 5. In the coating weight range 40–100%, as expected, an increase of the heating rate shifts the curves to higher temperatures. At residual weights below 40%, the heating rate dependence no longer holds, indicating that the material decomposition becomes unstable. We utilized the above-described approach for obtaining lifetime data from the dynamic TGA curves. Since the fiber failure criterion is unknown, we calculated the lifetimes that correspond to several weight losses, $F\%$: 5, 10, 25 and 50%.

1) *Selection of Weight Loss Range*: To apply (2)–(5), one must select the magnitudes of $X\%$ and $Y\%$ from the experimental weight loss curve (see Fig. 1). The selection is somewhat arbitrary as long as the selected range represents sufficient weight loss and the derivation of the corresponding temperatures is reliable. For example, for $F = 25\%$ one may use, say, $X = 10\%$ and $Y = 20\%$ or $X = 5\%$ and $Y = 25\%$. We recommend not to use $X < 5\%$. At $0 < X < 5\%$, the weight changes slowly, leading to a larger uncertainty in the determined value of $T_{\beta, X\%}$. For a given failure criterion $F\%$, we compared results using different magnitudes of $X\%$ and $Y\%$. Thus, for $F = 25\%$, we used a “narrower” range, $X = 10\%$ and $Y = 20\%$, and a “broader” one, $X = 5\%$ and $Y = 25\%$. Both $X\% - Y\%$ sets provided very similar predictions for the coating use temperature. Thus, the activation energies obtained for Coating A are 123 ± 5 and 124 ± 5 kJ/mol, for the narrower and broader ranges, respectively. For the same sets of $X\%$ and $Y\%$, the 20-year use temperatures were $94 + 6/-4$ and $93 + 6/-4$ °C, respectively. We see that the thermal decomposition of Coating A in air follows the same or similar dynamics through both of the $X\% - Y\%$ ranges. In general,

TABLE I
USE TEMPERATURES (°C) AND ARRHENIUS PARAMETERS FOR COATING A
IN AIR OBTAINED WITH DIFFERENT CRITERIA

Use Time	Criterion (Weight Loss at Failure)			
	5%	10%	25%	50%
20 Years	85 +13/-5	87 +9/-5	93 +6/-4	107 +6/-4
1 Year	111 +10/-5	114 +8/-4	122 +5/-3	139 +5/-4
1 Month	135 +8/-5	140 +7/-4	150 +4/-3	170 +4/-3
1 Day	174 +5/-4	181 +4/-3	195 +3/-2	221 +3/-2
1 Hour	217 +3/-2	229 +2/-2	247 +1/-1	279 +1/-1
1 Minute	288 +4/-3	306 +4/-3	333 +4/-3	379 +4/-3
E^* (kJ/mol)	133 ± 9	128 ± 7	124 ± 5	123 ± 5
R	0.9988	0.9992	0.9996	0.9996
$X\% - Y\%$ range	5% -10%	5% -15%	5% - 25%	10% - 50%

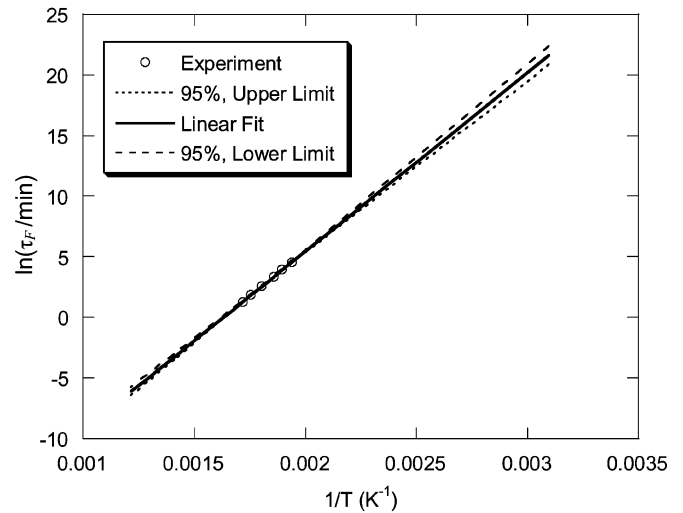


Fig. 6. Arrhenius plot for Coating A in air in coordinates of (5) for $F = 25\%$. The continuous line shows linear fit; the dashed and dotted lines show the lower and upper 95% confidence limits for the extrapolated values of $\ln \tau_r$.

it seems most reasonable to select a broader $X\% - Y\%$ range since it better represents the target weight loss range, i.e., from 0 to $F\%$. For consistency, we utilized the broader $X\% - Y\%$ range for $F = 25\%$ with all coating-gas systems. The $X\% - Y\%$ ranges used for $F = 5, 10,$ and 50% are listed at the bottom of Table I.

2) *Determination of Lifetime at Different Temperatures*: An example of the Arrhenius plots is shown in Fig. 6. This plot is obtained for Coating A in air, assuming a 25% coating weight loss criterion. As can be seen, the experimental points fall well on a straight line with a correlation coefficient of 0.9996. Table I presents the lifetime-temperature data obtained using different weight loss criteria. It is obvious from Table I that the “lifetime” is a function of two variables: the failure weight loss and the use temperature. Thus, if we assume that Fiber A fails to perform optically and mechanically at 25% coating weight loss, such fiber can sustain 20 years at 93 °C. It can also be used at higher

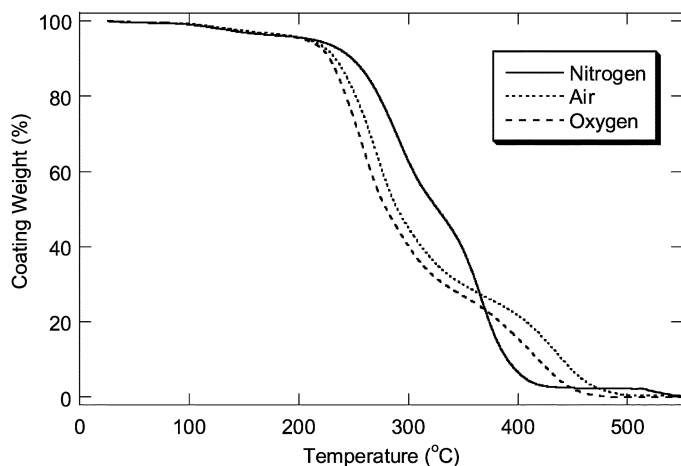


Fig. 7. Effects of the environment on thermal decomposition of Coating A. All three curves are obtained at a heating rate of 0.5 °C/min.

temperatures, but for shorter times. For example, this fiber will sustain 1 year at 122 °C and 1 month at 150 °C, again based on the 25% weight loss criterion.

If the fiber fails at a different weight loss level, say 10% weight loss, then the use temperatures will shift to lower magnitudes: 20 years at 87 °C, 1 year at 114 °C and 1 month at 140 °C. In contrast, if the fiber is known to fail at 50% coating weight loss, the use temperatures will be: 20 years at 107 °C, 1 year at 139 °C and 1 month at 170 °C.

Similar activation energies were obtained for the different weight loss ranges, despite the complicated shape of the DTG curves. It follows that the most critical decomposition steps that occur at residual weights above 50% have similar activation energies. However, this should not necessarily be true for other coating types.

3) *Environmental Effects*: Fig. 7 compares dynamic TGA curves obtained with different purge gases. As expected, thermal stability decreases in the following order: nitrogen > air > oxygen. Table II summarizes the lifetime-temperature data for Coating A in different environments assuming the 25% weight loss criterion. In nitrogen and oxygen, the Arrhenius data exhibited somewhat lower correlation coefficients and, as a consequence, the lifetime temperatures were obtained with larger uncertainties. Lower correlation coefficients may be a consequence of the associated chemical reactions having different activation energies. Experimental uncertainties may also contribute to the magnitude of the correlation coefficient.

4) *Results for Coatings B and C*: Table III shows the data obtained for Coatings B and C using the 25% weight loss criterion. Fig. 8 provides time-temperature diagrams for all studied coatings in air, using the same criterion. The error bars correspond to the uncertainties in evaluating the magnitudes of T and $\ln \tau_F$. With a diagram such as shown in Fig. 8, one can easily estimate the highest operation temperature (when the use time is known) or the “lifetime” of the fiber at the known use temperature. Both Table III and Fig. 8 clearly indicate that thermal stabilities of the coatings increase in the following sequence: Coating A (dual acrylate) < Coating B (fluoroacrylate polymer cladding) < Coating C (polyimide).

TABLE II
USE TEMPERATURES (°C) AND ARRHENIUS PARAMETERS FOR COATING A IN NITROGEN, AIR AND OXYGEN OBTAINED AT 25% WEIGHT LOSS CRITERION

Use Time	Gas Environment		
	Nitrogen	Air	Oxygen
20 Years	112 +27/-7	93 +6/-4	89 +12/-5
1 Year	141 +20/-7	122 +5/-3	117 +10/-5
1 Month	168 +15/-7	150 +4/-3	144 +8/-5
1 Day	213 +8/-5	195 +3/-2	188 +5/-4
1 Hour	264 +3/-3	247 +1/-1	238 +2/-2
1 Minute	348 +11/-8	333 +4/-3	321 +6/-4
E* (kJ/mol)	136 ± 15	124 ± 5	125 ± 8
R	0.9970	0.9996	0.9989
X%-Y% range	5% - 25%	5% - 25%	5% - 25%

TABLE III
USE TEMPERATURES (°C) AND ARRHENIUS PARAMETERS FOR COATINGS B AND C IN NITROGEN, AIR AND OXYGEN OBTAINED AT 25% WEIGHT LOSS CRITERION

Use Time	Coating B			Coating C		
	Nitrogen	Air	Oxygen	Nitrogen	Air	Oxygen
20 Years	201 +5/-3	124 +5/-3	100 +11/-5	375 +9/-5	251 +28/-9	222 +7/-5
1 Year	230 +4/-3	153 +5/-3	127 +9/-5	410 +7/-5	296 +22/-9	265 +6/-5
1 Month	256 +4/-3	180 +4/-3	153 +7/-4	443 +6/-4	340 +18/-9	307 +6/-4
1 Day	297 +2/-2	224 +3/-2	194 +5/-3	493 +3/-3	412 +11/-8	376 +4/-3
1 Hour	342 +1/-1	274 +1/-1	240 +2/-2	546 +1/-1	496 +4/-4	457 +2/-2
1 Minute	410 +2/-2	355 +3/-2	314 +4/-3	626 +4/-3	640 +12/-9	597 +4/-3
E* (kJ/mol)	208 ± 7	144 ± 5	138 ± 9	311 ± 15	165 ± 14	154 ± 5
R	0.9997	0.9995	0.9990	0.9992	0.9982	0.9997
X%-Y% range	10%-25%	5%-25%	5%-25%	5%-25%	5%-25%	5%-25%

B. Correlation With Optical Fiber Properties

To use the TGA data in lifetime predictions for specialty optical fibers, it is important to correlate the results of thermal analysis with the fiber performance. For instance, Cusanello *et al.* [43] reported in their investigation into similar polyimide-coated optical fibers that fiber strength dropped sharply in the time/temperature regime where we observe 25% wt. loss. Armed with the knowledge of the correlation, one can readily predict fiber performance using TGA data.

Comparison of Fiber Diameter Reduction With TGA Weight Loss:

In this paper, we investigated thermal aging effects on the coating diameter and strength of the fiber with Coating A. Dry

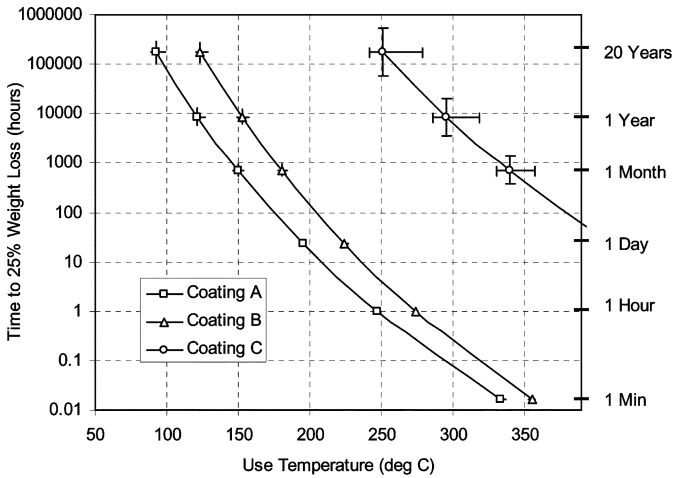


Fig. 8. Time-temperature diagrams for coatings A, B, and C in air (25% wt. loss criterion).

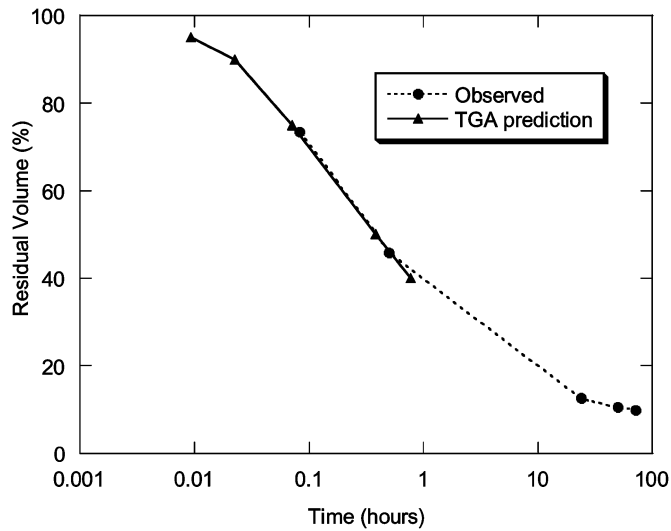


Fig. 9. Residual Coating A volume for a fiber aged at 300 °C in air. Solid curve is based on extrapolations of the TGA data.

aging of fibers was performed using an oven at 300 °C, where the aging times were 5 and 30 min, and 24, 50, and 72 h. From the measured coating diameter and the glass diameter (125 μm), the residual coating volume was calculated. These magnitudes (expressed in percent of the “as drawn” coating volume) are shown in Fig. 9.

The decrease of the coating volume is related to the thermal decomposition of the coatings. At the longest exposure, only 10.5% of the initial volume is retained by Coating A. Upon aging, the fiber color became progressively darker, from yellowish (after 5 min) to brown to black (after 30 min). No cracks or other defects were evident at the coating surface at least up to 30 min. After 24 h (and > 75% volume loss), we observed about 1 crack per 5 cm.

It is of interest to compare these data with predictions from our TGA approach. Based on the TGA data, we calculated the times needed for Coating A to lose 5, 10, 25, 50, and 60% of its initial weight. We were not able to calculate the times for higher weight losses because of the inconsistency of the dynamic TGA curves in that weight loss range (see Fig. 5). For simplicity, we assume that the coating density does not change significantly

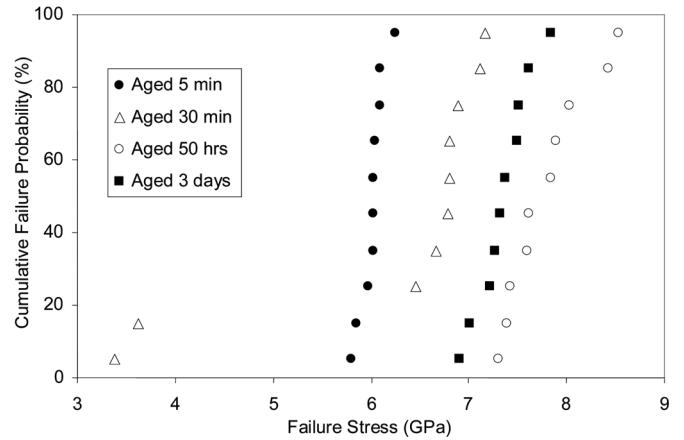


Fig. 10. Distribution of the failure stress observed for Fiber A aged at 300 °C for 5 min, 30 min, 50 h, and 3 days.

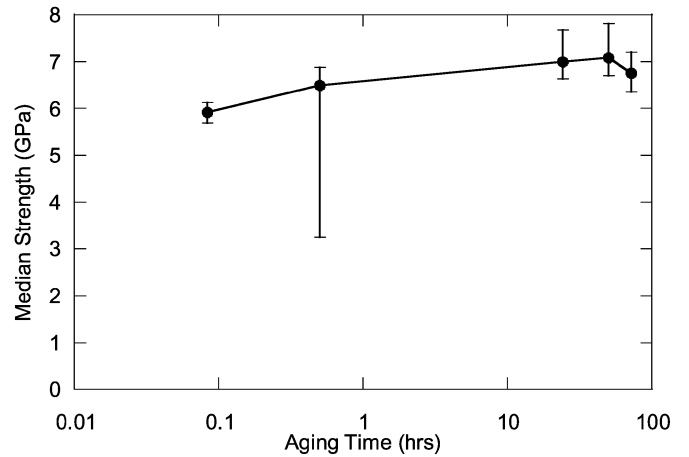


Fig. 11. Median strength of optical fibers aged at 300 °C, measured by the 2-point bend test method. The Error bars correspond to the lowest and highest magnitudes determined at each condition.

upon its decomposition, so the weight loss percentage is equivalent to the volume change percentage. The TGA-based prediction is compared with the experimental data in Fig. 9. Indeed, good agreement is observed.

1) *Coating Degradation and Fiber Strength:* Fiber A as drawn and aged at 300 °C, as described above, was tested for strength using the two-point bend test method. Fig. 10 shows some of the obtained failure probability distributions. For most of the aged fibers, the observed distributions are relatively narrow, exhibiting Weibull slopes in the range between 20 and 60. The median failure stress and the ranges of the obtained magnitudes are shown in Fig. 11. It can be seen that the fibers become stronger upon thermal aging, at least up to aging time of 50 h. Such trend is counter-intuitive, especially keeping in mind that the coatings lose up to 90% of their volume (see Fig. 9). A subtle median strength decrease seemed to be observed after 72 hours. At this point, the coating had not only developed a few cracks, but it had visibly flaked off in several spots.

It follows that the fiber strength (at least measured for relatively small pieces of fiber, aged under static zero-stress conditions), is not an early indicator of failure at high temperatures. It is believed, however, that if the aging is prolonged, then below a certain coating thickness the fiber strength would degrade.

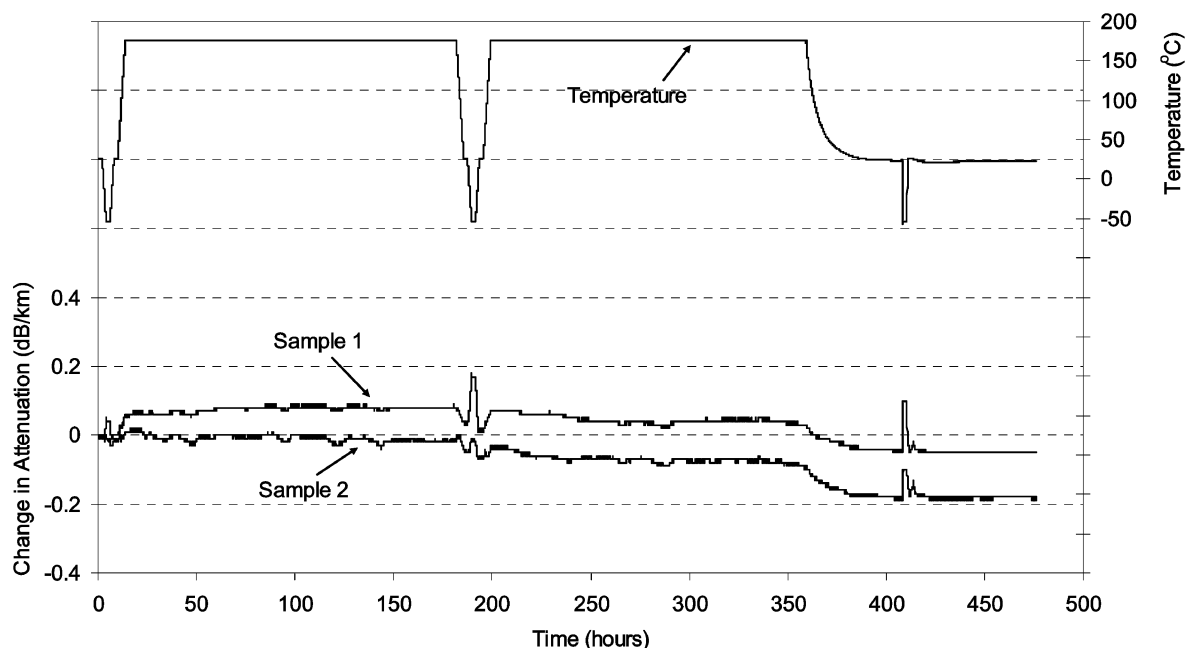


Fig. 12. Effects of thermal exposure on attenuation of Fiber A at 850 nm.

2) *Coating Color*: Our observations indicate that it is not always obvious how to define the fiber failure criterion. If, for instance, it is important for Fiber A to preserve its color, then a 5 min exposure to 300 °C might be considered as failure, which corresponds to $\sim 25\%$ weight loss. However, if fiber strength is considered the key factor, then the failure criterion might correspond to a weight loss above 90%.

3) *Strip Force and Modulus*: One previous study on a different acrylate coating system has shown that weight loss of $< 5\%$ can correspond to significant changes in primary coating strip force and modulus [10]. An increased modulus, in turn, tends to increase optical attenuation at low temperatures.

4) *Fiber Attenuation*: We have studied thermal aging effects on optical attenuation for the fiber with Coating A. Two identical 1-km fiber coils (samples 1 and 2) were subjected to thermal aging with continuous optical monitoring (850 nm) at 175 °C as follows (Fig. 12). First, the fiber was conditioned at room temperature, then cycled to -55 °C to assess baseline attenuation with unaged coating. The fiber was then ramped to 175 °C and held for 1 week. The effect on low-temperature attenuation was checked by an excursion to -55 °C, followed by a 2nd week at 175 °C. Finally, the fiber was allowed to cool slowly to room temperature, and the -55 °C attenuation was again checked.

As can be seen, fiber with Coating A experienced less than 0.2 dB/km increase in attenuation throughout the test. For most specialty fiber applications, this attenuation is acceptable. The changes in coating weights corresponding to 2 weeks at 175 °C were estimated from the TGA data to be in the range 34–38 wt%. It follows that even a significant coating weight loss does not necessarily hinder optical transmission.

VI. CONCLUSIONS

The concept of “thermal stability” as applied to specialty optical fibers includes three important aspects: performance acceptance criteria, continuous use time and upper use temperature. Only two of these three aspects are independent; e.g., knowing

the failure criterion and the continuous use time one should be able to deduce the upper use temperature. The fiber failure criterion fully depends on the application requirements. A relationship between the use time and the temperature can be obtained from dynamic thermogravimetric analysis of the fiber coating. Extrapolation of TGA data enables one to anticipate the fiber failure at various time/elevated temperature conditions.

ACKNOWLEDGMENT

The authors would like to thank D. Burgess and B. Slyman for drawing the fibers and R. Heinemann, K. Marceau, and R. Dyer for collecting the strength and attenuation data.

REFERENCES

- [1] J. T. Chapin, A. G. Hardee Jr, L. M. Larsen-Moss, C. M. Leshe, B. J. Overton, J. W. Shea, C. R. Taylor, and J. M. Turnipseed, “Optical transmission media and methods of making same,” U.S. Patent 4962992, 1990.
- [2] U. C. Paek, “Free drawing and polymer coating of silica glass optical fibers,” *Trans. ASME*, vol. 121, pp. 774–788, 1999.
- [3] S. R. Schmid and A. F. Toussaint, “Optical fiber coatings,” in *Specialty Optical Fibers Handbook*, A. Mendez and T. F. Morse, Eds. New York: Elsevier, 2007, pp. 95–122.
- [4] D. Glöge, “Optical fiber packaging and its influence on fiber straightness and loss,” *Bell Syst. Tech. J.*, vol. 54, pp. 245–262, 1975.
- [5] M. J. Sandelin and U. W. Gedde, “Long-term performance of cables based on chlorosulphonated polyethylene,” *Polym. Degrad. Stab.*, vol. 86, pp. 331–338, 2004.
- [6] P. Budrugaec, “On the evaluation of the thermal lifetime of polymeric materials which exhibit complex mechanism of thermal degradation consisting of two successive reactions,” *Polym. Degrad. Stab.*, vol. 67, pp. 271–278, 2000.
- [7] *Optical fibres—part 1–51: Measurement methods and test procedures—dry heat*, Int. Std. 60793-1-51 IEC:2001, Int. Electrotech. Commission, 2001.
- [8] *Polymeric materials—long term property evaluations*, UL Std. 746B, Rev. 3, Underwriters Lab., 1996.
- [9] M. G. Chan, D. A. Simoff, and I. P. Heyward, “Thermo-oxidative degradation and stabilization of UV-cured coatings,” in *Proc. ACS Div. Polym. Mat. Sci. Eng.*, 1988, vol. 58, pp. 204–208.
- [10] D. A. Simoff, M. G. Chan, J. T. Chapin, and B. J. Overton, “Thermo-oxidative aging of a primary lightguide coating in films and dual coated fibers,” *Polym. Eng. Sci.*, vol. 29, pp. 1177–1181, 1989.

- [11] H. Nakatani, S. Suzuki, T. Tanaka, and M. Terano, "New kinetic aspects on the mechanism of thermal oxidative degradation of polypropylenes with various tacticities," *Polymer*, vol. 46, pp. 12366–12371, 2005.
- [12] A. Saccani, A. Motori, and G. C. Montanari, "Short-term thermal endurance evaluation of thermoplastic polyesters by isothermal and non-isothermal thermogravimetric analysis," *J. Appl. Polym. Sci.*, vol. 98, pp. 698–973, 2005.
- [13] B. A. Howell and J. A. Ray, "Comparison of isothermal and dynamic methods for the determination of activation energy by thermogravimetry," *J. Therm. Anal. Calorim.*, vol. 83, pp. 63–66, 2006.
- [14] Y. N. Gupta, A. Chakraborty, G. D. Pandey, and D. K. Setua, "Thermal and thermooxidative degradation of engineering thermoplastics and life estimation," *J. Appl. Polym. Sci.*, vol. 92, pp. 1737–1748, 2004.
- [15] P. S. G. Krishnan and S. Veeramani, "Effects of methyl group substitution in the diamine and copolymer composition on thermal degradation of copolyimides based on 2,2-bis(3,4-dicarboxyphenyl) hexafluoropropane dianhydride," *Polym. Degrad. Stab.*, vol. 81, pp. 225–232, 2003.
- [16] Z. Peng and L. X. Kong, "A thermal degradation mechanism of poly(vinyl alcohol/silica nanocomposites)," *Polym. Degrad. Stab.*, vol. 92, pp. 1061–1071, 2007.
- [17] A. Mohamed, S. H. Gordon, and G. Biresaw, "Polycaprolactone/polystyrene bioblends characterized by thermogravimetry, modulated differential scanning calorimetry and infrared photoacoustic spectroscopy," *Polym. Degrad. Stab.*, vol. 92, pp. 1177–1185, 2007.
- [18] M. D. Fernandez, M. J. Fernandez, and P. Hoces, "Synthesis of poly(vinyl butyral)s in homogeneous phase and their thermal properties," *J. Appl. Polym. Sci.*, vol. 102, pp. 5007–5017, 2006.
- [19] G. Wei, D. Hua, and L. Gu, "Thermal stability of poly(ethylene-co-trimethylene terephthalate)s," *J. Appl. Polym. Sci.*, vol. 101, pp. 3330–3335, 2006.
- [20] L. F. Campo, F. S. Rodembusch, and V. Stefani, "New fluorescent monomers and polymers displaying an intramolecular proton-transfer mechanism in the electronically excited state. III. Thermogravimetric stability study of the benzazolyvinylene derivatives," *J. Appl. Polym. Sci.*, vol. 99, pp. 495–500, 2006.
- [21] J. Macan, I. Brnardic, S. Orlic, H. Ivankovic, and M. Ivankovic, "Thermal degradation of epoxy-silica organic-inorganic hybrid materials," *Polym. Degrad. Stab.*, vol. 91, pp. 122–127, 2006.
- [22] H. Kumar, A. A. Kumar, and Siddaramaiah, "Physico-mechanical, thermal and morphological behavior of polyurethane/poly(methyl methacrylate) semi-interpenetrating polymer networks," *Polym. Degrad. Stab.*, vol. 91, pp. 1097–1104, 2006.
- [23] M.-H. Yang, "On the thermal degradation of poly(styrene sulfones). VII. Evaluations of poly(styrene sulfone) thermal stability using invariant kinetic parameters," *J. Appl. Polym. Sci.*, vol. 85, pp. 1698–1705, 2002.
- [24] X. Ramis, J. M. Salla, and J. Puiggali, "Kinetic studies on the thermal polymerization of n-chloroacetyl-11-aminoundecanoate potassium salt," *J. Polym. Sci. A: Polym. Chem.*, vol. 43, pp. 1166–1176, 2005.
- [25] X. Meng, Y. Huang, H. Yu, and Z. Lv, "Thermal degradation kinetics of polyimide containing 2,6-benzobisoxazole units," *Polym. Degrad. Stab.*, vol. 92, pp. 962–967, 2007.
- [26] K. Chrissafis, K. M. Paraskevopoulos, and D. N. Bikiaris, "Effect of molecular weight on thermal degradation mechanism of the biodegradable polyester poly(ethylene succinate)," *Thermochim. Acta*, vol. 440, pp. 166–175, 2006.
- [27] B. Liu, Y. Li, L. Zhang, W. Yan, and S. Yao, "Thermal degradation kinetics of poly(N-adamantyl-exo-nadimide) synthesized by addition polymerization," *J. Appl. Polym. Sci.*, vol. 103, pp. 3003–3009, 2007.
- [28] H. H. Horowitz and G. Metzger, "A new analysis of thermogravimetric traces," *Anal. Chem.*, vol. 35, pp. 1464–1468, 1963.
- [29] A. W. Coats and J. P. Redfern, "Kinetic parameters from thermogravimetric data," *J. Polym. Sci., Polym. Lett.*, vol. 3, pp. 917–920, 1965.
- [30] A. Broido, "A simple, sensitive graphical method of treating thermogravimetric analysis data," *J. Polym. Sci. Pt. A*, vol. 7, pp. 1761–1773, 1969.
- [31] T. Ozawa, "A new method of analyzing thermogravimetric data," *Bull. Chem. Soc. Jpn.*, vol. 38, pp. 1881–1886, 1965.
- [32] J. H. Flynn and L. A. Wall, "A quick, direct method for the determination of activation energy from thermogravimetric data," *J. Polym. Sci. Polym. Lett.*, vol. 4, pp. 323–328, 1966.
- [33] H. E. Kissinger, "Reaction kinetics in differential thermal analysis," *Anal. Chem.*, vol. 29, pp. 1702–1706, 1957.
- [34] H. L. Friedman, "Kinetics of thermal degradation of char-forming plastics from thermogravimetry. Application to a phenolic plastic," *J. Polym. Sci., Pt. C*, vol. 6, pp. 183–195, 1964.
- [35] B. J. Holland and J. N. Hay, "The value and limitations of non-isothermal kinetics in the study of polymer degradation," *Thermochim. Acta*, vol. 388, pp. 253–273, 2002.
- [36] T.-H. Liou, "Kinetics study of thermal decomposition of electronic packaging material," *Chem. Eng. J.*, vol. 98, pp. 39–51, 2004.
- [37] A. Gu and G. Liang, "Thermal stability of epoxy resin by thermogravimetric analysis," *Thermochim. Acta*, vol. 412, pp. 139–147, 2004.
- [38] L. L. C. Guan, A. Zhang, D. Chen, and Z. Qing, "Thermal stabilities and the thermal degradation kinetics of polyimides," *Polym. Degrad. Stab.*, vol. 84, pp. 31–39, 2004.
- [39] X. Chen, J. Yu, and S. Guo, "Thermal oxidative degradation kinetics of PP and PP/Mg(OH)₂ flame retardant composites," *J. Appl. Polym. Sci.*, vol. 89, pp. 1530–1536, 2003.
- [40] N. R. Draper and H. Smith, *Applied Regression Analysis*. New York: Wiley, 1966.
- [41] M. J. Matthewson, C. R. Kurkjian, and S. T. Gulati, "Strength measurement of optical fibers by bending," *J. Amer. Ceram. Soc.*, vol. 69, pp. 815–821, 1986.
- [42] J. L. Mrotek, M. J. Matthewson, and C. R. Kurkjian, "Diffusion of moisture through fatigue and aging-resistant polymer coatings on light-guide fibers," *J. Lightw. Technol.*, vol. 21, pp. 1775–1778, 2003.
- [43] V. A. Cusanello, N. J. Jacobson, M. V. Supczak, and P. R. Stupak, "A hermetic coating combination for adverse environments," in *Proc. Int. Wire & Cable Symp.*, 1995, pp. 335–342.



Andrei Stolov received the Ph.D. degree in physics in 1985 from Kazan State University, Russia.

He was a Senior Research Fellow with the Department of Chemistry, Kazan State University. He subsequently held positions as a Visiting Scientist at RUCA University, Antwerp, Belgium, and as a Postdoctoral Fellow with the Polymer Science and Engineering Department, University of Massachusetts, Amherst. In 2000, he joined Lucent Technologies (now OFS), Avon, CT, as a Member of Technical Staff, where his focus has been the

development and characterization of polymer coatings for specialty optical fibers. He has authored more than 90 publications in the fields of molecular spectroscopy and polymer science.



Debra Simoff received the M.S. degree in polymer science and engineering from the University of Massachusetts, Amherst.

In 1982, she joined AT&T Bell Laboratories, Murray Hill, NJ, as a Member of Technical Staff, conducting applied research related to polymers and coatings used in telecommunications. She transitioned within AT&T to Lucent Technologies (now OFS), joining the Specialty Photonics Division, Avon, CT, in 2000 as Supervisor of the Coatings and Polymer Materials Group. She currently supports

the development of specialty optical fiber products and processes. She is a co-inventor of six U.S. patents related to specialty coatings for the fabrication of fiber Bragg gratings.



Jie Li received the Ph.D. degree in ceramic science and engineering in 1996 from Rutgers University, New Brunswick, NJ.

He then joined Spectran Specialty Optics (now OFS Specialty Photonics Division, Avon, CT) as a Fiber Preform Engineer. He is currently Senior Manager of Operations and Engineering for Fiber and Cable. He has authored numerous journal publications and technical presentations in the fields of defects in glass, optical fibers, and fiber materials.